



## Propagation of back-arc extension into the arc lithosphere in the southern New Hebrides volcanic arc

M. Patriat, J. Collot, L. Danyushevsky, M. Fabre, S. Meffre, T. Falloon, P. Rouillard, B. Pelletier, M. Roach, Marc Fournier

### ► To cite this version:

M. Patriat, J. Collot, L. Danyushevsky, M. Fabre, S. Meffre, et al.. Propagation of back-arc extension into the arc lithosphere in the southern New Hebrides volcanic arc. *Geochemistry, Geophysics, Geosystems*, 2015, 16 (9), pp.3142-3159. 10.1002/2015GC005717 . hal-01365909

**HAL Id: hal-01365909**

**<https://hal.science/hal-01365909>**

Submitted on 20 Dec 2021

**HAL** is a multi-disciplinary open access archive for the deposit and dissemination of scientific research documents, whether they are published or not. The documents may come from teaching and research institutions in France or abroad, or from public or private research centers.

L'archive ouverte pluridisciplinaire **HAL**, est destinée au dépôt et à la diffusion de documents scientifiques de niveau recherche, publiés ou non, émanant des établissements d'enseignement et de recherche français ou étrangers, des laboratoires publics ou privés.

Copyright



# Geochemistry, Geophysics, Geosystems

## RESEARCH ARTICLE

10.1002/2015GC005717

### Special Section:

Assessing Magmatic, Neovolcanic, Hydrothermal, and Biological Processes along Intra-Oceanic Arcs and Back-Arcs

### Key Points:

- Back-arc extension then spreading ridge propagates in the S Vanuatu volcanic arc
- Rifting then drifting cause arc bits to be isolated within back-arc domain
- Very primitive subduction related magmas characterize such extensional settings

### Supporting Information:

- Supporting Information S1
- Table S1

### Correspondence to:

M. Patriat,  
martin.patriat@ifremer.fr

### Citation:

Patriat, M., J. Collot, L. Danyushevsky, M. Fabre, S. Meffre, T. Falloon, P. Rouillard, B. Pelletier, M. Roach, and M. Fournier (2015), Propagation of back-arc extension into the arc lithosphere in the southern New Hebrides volcanic arc, *Geochem. Geophys. Geosyst.*, 16, 3142–3159, doi:10.1002/2015GC005717.

Received 9 JAN 2015

Accepted 25 JUL 2015

Accepted article online 1 AUG 2015

Published online 24 SEP 2015

## Propagation of back-arc extension into the arc lithosphere in the southern New Hebrides volcanic arc

M. Patriat<sup>1,2</sup>, J. Collot<sup>2</sup>, L. Danyushevsky<sup>3</sup>, M. Fabre<sup>1,2</sup>, S. Meffre<sup>3</sup>, T. Falloon<sup>4</sup>, P. Rouillard<sup>5</sup>, B. Pelletier<sup>6</sup>, M. Roach<sup>3</sup>, and M. Fournier<sup>7</sup>

<sup>1</sup>IFREMER, Nouméa, New Caledonia, <sup>2</sup>Service Géologique de Nouvelle-Calédonie, Nouméa, New Caledonia, <sup>3</sup>ARC Centre of Excellence in Ore Deposits, University of Tasmania, Hobart, Australia, <sup>4</sup>School of Physical Sciences, University of Tasmania, Hobart, Tasmania, Australia, <sup>5</sup>ADECAL-Technopole, ZoNéCo Research Program, Nouméa, New Caledonia, <sup>6</sup>IRD, Nouméa, New Caledonia, <sup>7</sup>Institut des Sciences de la Terre de Paris, CNRS UMR 7193, Université Pierre and Marie Curie, Paris, France

**Abstract** New geophysical data acquired during three expeditions of the R/V Southern Surveyor in the southern part of the North Fiji Basin allow us to characterize the deformation of the upper plate at the southern termination of the New Hebrides subduction zone, where it bends eastward along the Hunter Ridge. Unlike the northern end of the Tonga subduction zone, on the other side of the North Fiji Basin, the 90° bend does not correspond to the transition from a subduction zone to a transform fault, but it is due to the progressive retreat of the New Hebrides trench. The subduction trench retreat is accommodated in the upper plate by the migration toward the southwest of the New Hebrides arc and toward the south of the Hunter Ridge, so that the direction of convergence remains everywhere orthogonal to the trench. In the back-arc domain, the active deformation is characterized by propagation of the back-arc spreading ridge into the Hunter volcanic arc. The N-S spreading axis propagates southward and penetrates in the arc, where it connects to a sinistral strike-slip zone via an oblique rift. The collision of the Loyalty Ridge with the New Hebrides arc, less than two million years ago, likely initiated this deformation pattern and the fragmentation of the upper plate. In this particular geodynamic setting, with an oceanic lithosphere subducting beneath a highly sheared volcanic arc, a wide range of primitive subduction-related magmas has been produced including adakites, island arc tholeiites, back-arc basin basalts, and medium-K subduction-related lavas.

## 1. Introduction

Numerical and laboratory experiments of subduction zones and measurements of shear wave anisotropy have emphasized the 3-D complexity of the mantle flow occurring at a slab edge [Smith *et al.*, 2001; Kincaid and Griffiths, 2003; Schellart, 2004; Funicello *et al.*, 2006; Schellart *et al.*, 2007; Kneller and van Keken, 2008; Long and Silver, 2008; Jadamec and Billen, 2010]. In such settings, the presence of a strong toroidal component of the mantle flow, which forces material around the slab edge, has important consequences for the dynamics, temperature, and composition of the mantle wedge. The geometry of the slab edge, including the location of slab tears, also determines the pathways for the asthenosphere from under the subducted slab to flow into the mantle wedge above the slab. This in turn affects the dynamics of the upper plate, and the nature and distribution of arc and back-arc volcanism [Hole *et al.*, 1991; Cole and Stewart, 2009; Thorkelson and Breitsprecher, 2005; Thorkelson *et al.*, 2011].

The subduction termination at the southern end of the New Hebrides subduction zone is an example where such complex 3-D processes occur, resulting in a diverse range of primitive subduction related magmas [Monzier *et al.*, 1993, 1997; Sigurdsson *et al.*, 1993; Danyushevsky *et al.*, 2006, 2008; Durancie *et al.*, 2012].

However, the tectonic setting, plate boundaries, and the geometry of the lithospheric slab are poorly known on the southwestern edge of the North Fiji Basin. Although the Wadati-Benioff plane clearly defines the New Hebrides subducting slab up to 22°S, farther south the slab geometry is poorly constrained [Pascal *et al.*, 1978; Coudert *et al.*, 1981; Louat, 1982; Monzier *et al.*, 1984, 1989; Louat *et al.*, 1988; Richards *et al.*, 2011; Lister *et al.*, 2012], and the exact location of the slab edge is not known.

The lack of geophysical constraints at depth combined with the complex fragmentation of the upper plate [Louat and Pelletier, 1989; Maillet *et al.*, 1989; Monzier *et al.*, 1997; Pelletier *et al.*, 1998] makes it difficult to

obtain a comprehensive pattern of plate motions, and makes attempts at defining subduction parameters back in time problematic [Lister *et al.*, 2012]. However, a better knowledge of the slab geometry east of 171°E would help to understand the petrogenesis of the volcanism which occurs in this area.

In this paper, we describe a new set of geophysical data, including multibeam bathymetry, acquired in the southwestern part of the North Fiji Basin (NFB) during three surveys of the R/V Southern Surveyor in 2004, 2006, and 2009. The new data reveal the active deformation in the upper plate and shows the propagation of back-arc extension in the Hunter volcanic arc above the subducting Australian plate. We use these data to reassess the geometry of the slab at depth, and to infer the tectonic processes affecting the southern part of the NFB. In particular, the new geophysical data demonstrate the propagation of back-arc extension into the pre-existing arc directly above the present-day subducting plate, resulting in continuous disintegration of the arc lithosphere. We focus on the tectonic process while the geochemistry of magmatic rocks within this area will be discussed elsewhere.

## 2. Tectonic Setting

The E-W relative convergence between the Australian and Pacific plates is taken up by westward subduction of the Pacific plate along the Tonga-Kermadec subduction zone and eastward subduction of the Australian plate along the New Hebrides and Puysegur subduction zones (Figures 1a and 1b). Along the New Hebrides subduction zone, the Australian slab of late Eocene age [Mortimer *et al.*, 2014] sinks beneath the North Fiji Basin (NFB), a marginal basin aged ~10 Ma [Auzende *et al.*, 1988]. The transition from the New Hebrides to the Tonga-Kermadec subduction zones is achieved through the left-lateral Fiji Fracture zone, a complex succession of ridges and faults mostly N-S to NE-SW and E-W, respectively [Pelletier *et al.*, 1998]. Because of the latitudinal overlapping of the two opposite subduction zones, the strike-slip motion along the Fiji Fracture Zone is supplemented by extension distributed over and between two back-arc basins, the North Fiji and Lau basins (Figure 1a). The deformation pattern of this wide area is therefore characterized by sinistral transtension whose expression is often schematized as an alternation of N-S spreading axes and east west sinistral faults, but whose actual expression (Figure 1a) is somewhat more complex [Auzende *et al.*, 1988; Louat and Pelletier, 1989; Pelletier and Louat, 1989; Pelletier *et al.*, 1998].

Because of the sparsity of geophysical and bathymetric data, the connection of the southern extremity of NFB Central Spreading Ridge with the New Hebrides subduction zone is not clear, resulting in a variety of tectonic model being proposed as follows:

1. Maillet *et al.* [1989] suggested the N-S accretion axis propagates obliquely toward the southwest.
2. Pelletier *et al.* [1998] proposed that an E-W sinistral strike-slip system connects the N-S accretion axis to the East (this hypothesis is presented in Figure 1a).
3. Monzier [1993] suggested that a triple junction exists somewhere along the Central Spreading Ridge sharing the motion between an E-W sinistral strike-slip system and a prolongation of the N-S accretion axis toward the southwest.

### 2.1. Present Day Seismotectonics at the Southern Termination of the New Hebrides Subduction Zone

At their termination, a sharp 90° bend characterizes both the Tonga and New Hebrides subduction zones. In Tonga, where it is well documented, this bend is accompanied by an abrupt switch of the nature of the boundary between the Pacific and Tonga plates (Figure 1). This is attested by the unequivocal spatial distribution and nature of seismic events [Pelletier and Louat, 1989; Millen and Hamburger, 1998] as well as by the geometry of the subducted slab as revealed by seismic tomography [Wortel *et al.*, 2009]. The plate boundary accommodates frontal subduction south of 16°S, while it corresponds to a sinistral E-W transform fault north of 15°S [Millen and Hamburger, 1998]. At the subduction termination, the Pacific plate (red plate on 3-D sketch in Figure 1c) separates in two, the northern side is staying flat at the surface and wrenches along the North Fiji Basin, while the southern side is subducting down below the Lau Basin. The distribution of the seismicity is consistent with this kinematic setting: seismicity along the Wadati-Benioff plane stops abruptly thereby defining a slab edge that can be tracked almost linearly from a depth of 600 km to the surface. Very locally, where the Pacific Plate separates in two and around 30–80 km at depth (green area on 3-D sketch in Figure 1), specific earthquake swarms results from the hypothesized tearing of the lithosphere (these particular swarms have a vertical focal plane [Millen and Hamburger, 1998]).

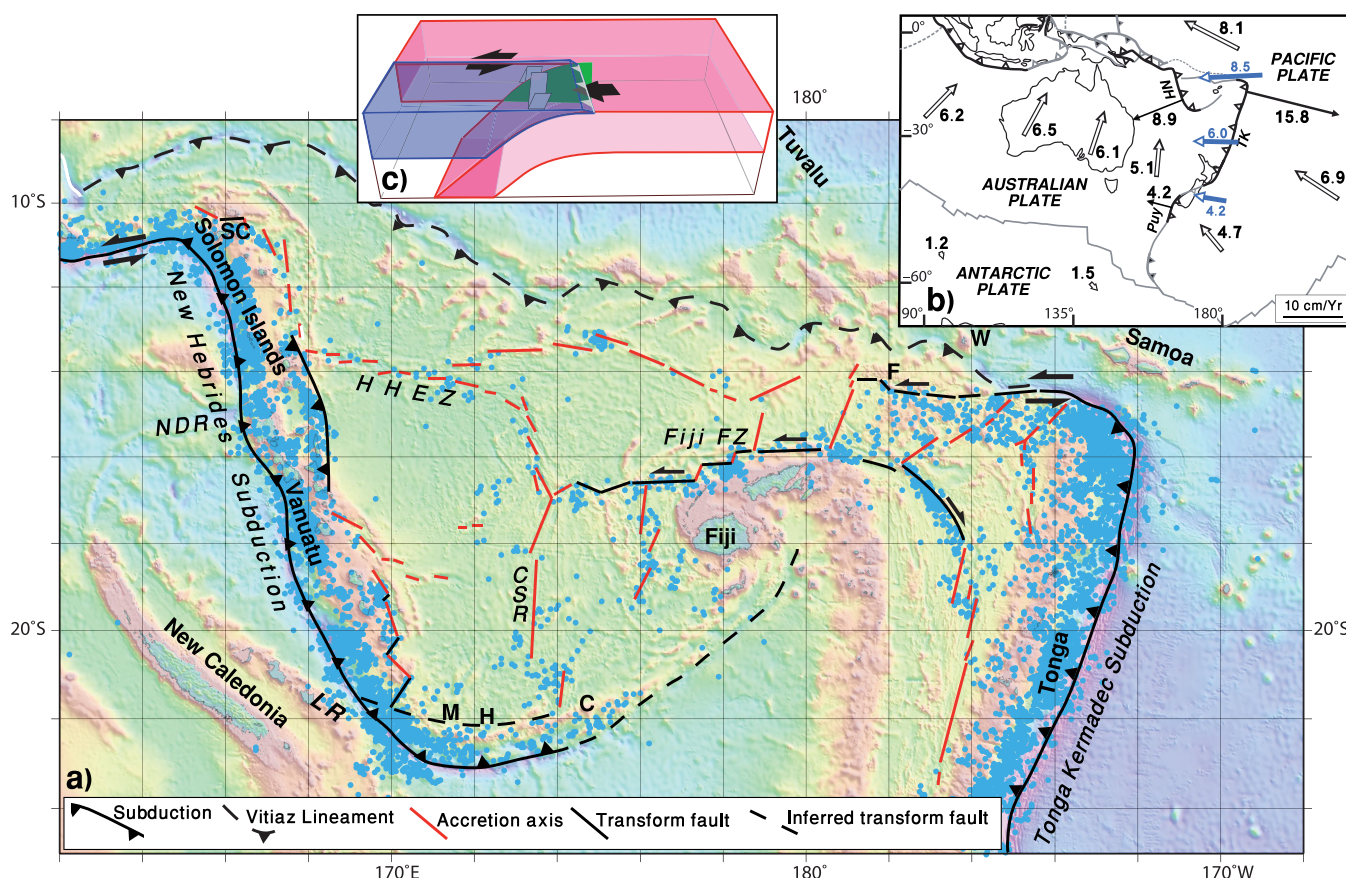


**Figure 1.** (a) Tectonic setting of the North Fiji Basin after Pelletier [1999]. The background depicts satellite bathymetry [Smith and Sandwell, 1997]. Blue circles are shallow (<50 km) earthquakes from the USGS catalogue: C, Conway Reef; CSR, Central Spreading ridge; Fiji FZ, Fiji Fracture zone; F, Futuna; H, Hunter; HHEZ, Hazel Holme Extensional Zone; LR, Loyalty ridge; M, Matthew; NDR, North D'Entrecasteaux Ridge; SC, Santa Cruz; W, Wallis. The two red stars correspond to inflection point of the New Hebrides and Tonga subductions used as reference for distances in Figure 3 (see text). (b) Inset map shows plate velocities in the hotspot reference frame (open arrows) and trench migration velocities (black arrows): NH, New Hebrides; Puy, Puysegur; TK, Tonga Kermadec (see Schellart *et al.* [2007], from which this map is drawn, for more references). Blue arrows are velocity of Pacific relative to Australia according to MORVEL [DeMets *et al.*, 2010]. (c) The inset 3-D sketch illustrates the shift from subduction to strike-slip characterizing the northern termination of the Tonga subduction, [After Govers and Wortel, 2005].

In contrast to Tonga, we know from the distribution and nature of the seismicity [Louat, 1982; Louat *et al.*, 1988; Louat and Pelletier, 1989; Pelletier *et al.*, 1998] and from GPS measurements [Calmant *et al.*, 1995, 1997, 2000, 2003; Taylor *et al.*, 1995] that the New Hebrides subduction southern termination is not characterized by such a subduction-to-transform transition (Figure 2). Unlike the seismic events distribution observed at the northern termination of the Tonga subduction, thrust-type earthquakes, with P axes perpendicular to the trench axis, exist as far East as 174°E, far beyond the New Hebrides subduction bend. The rotation of the thrust-type events P axes is gradual and accompanies the rotation of the trench axis. P axes thereby remain perpendicular to the trench (Figure 3). Consequently, the subduction is perpendicular to the trench without any noticeable obliquity from its northwestern end, around 165°E, all the way to 174°E.

This rotation of the convergence direction at the southern end of the New Hebrides subduction is confirmed by GPS measurements of the relative movements of volcanic islands within the NFB and the Australian plate [Calmant *et al.*, 1995, 2000, 2003]. At each of these locations, the relative movements measured by GPS are normal to the trench axis.

Finally, Monzier *et al.* [1984, 1989, 1990] demonstrated, from a comprehensive analysis of data (including seabed morphology, multibeam data, submersible dives, the nature of earthquakes and their distribution), that thrusting of the Loyalty Ridge under the New Hebrides arc has resulted in a recent collision in this area.

## 2.2. Geometry of the Australian Slab Along the New Hebrides Subduction Zone

The geometry of the slab, especially its lateral extent and downdip length, can be deduced from the depth of intermediate (50–400 km) earthquakes. Deeper events also occur in this area but their origin is beyond



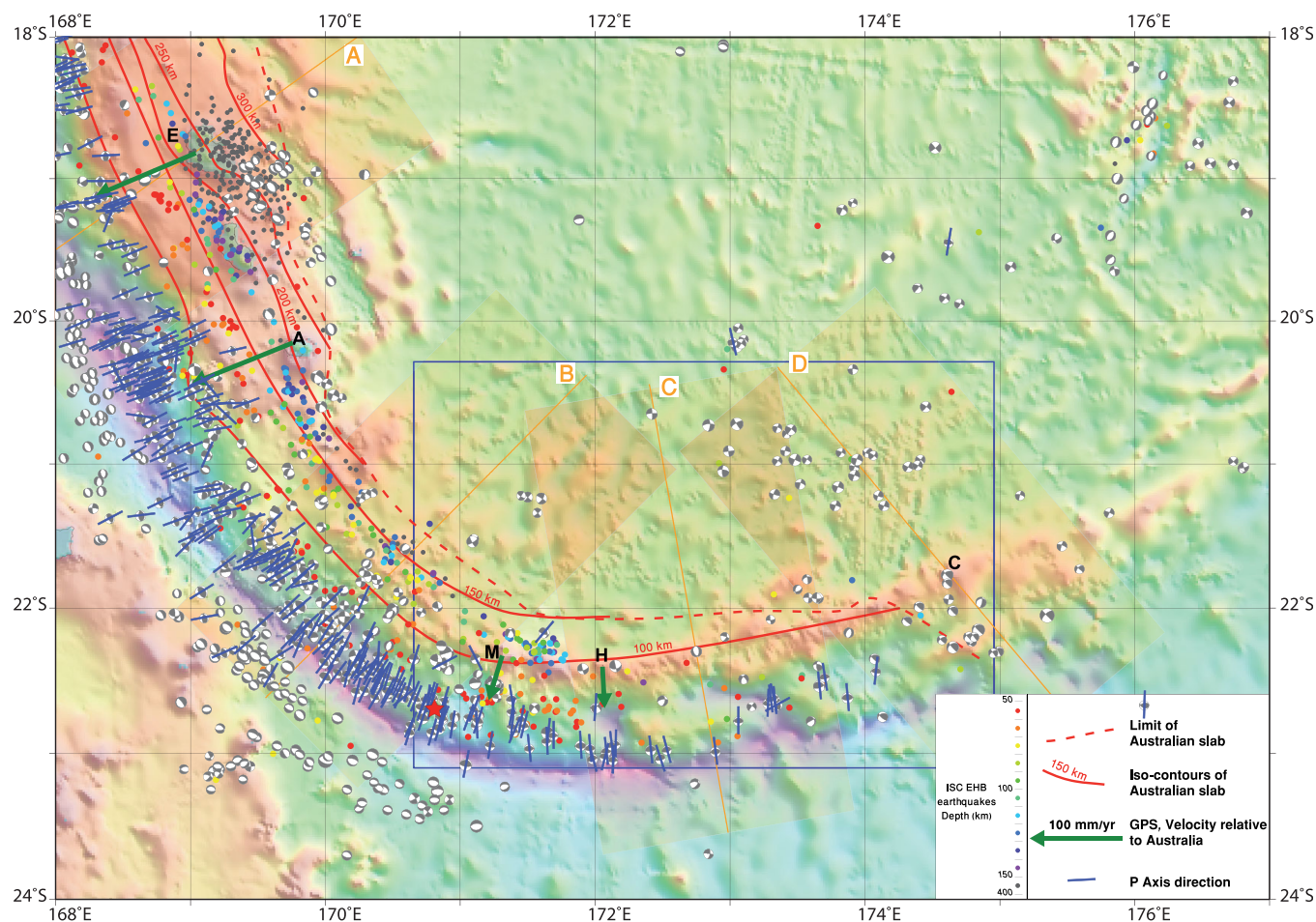


**Figure 2.** Seismotectonics of the southern termination of the New Hebrides subduction. Focal mechanism solutions from the CMT Global Project [Ekström *et al.*, 2012] for earthquakes shallower than 80 km are reported, with thrust faults P-axis direction in blue. Intermediate hypocenters ( $50 \text{ km} < z < 150 \text{ km}$ ) from the ISC EHB bulletin [Engdahl *et al.*, 1998] are reported as color coded circles (color scale in the legend). Background is the satellite topography from Smith and Sandwell [1997]. GPS measurements from Calmant *et al.* [2003] are indicated (green arrows) for four islands. A, Aneytum; E, Erromango; H, Hunter; M, Matthew. Orange lines with their label correspond to profiles in Figure 2. Transparent orange areas around these profiles indicate the 150 km wide zone where hypocenters were selected for projection. The small red star corresponds to inflection point of the New Hebrides subduction used as reference for distances in Figure 3 (see text). C, Conway.

the scope of this paper [see Hamburger and Isacks, 1987; Okal and Kirby, 1998; Brudzinski and Chen, 2003; Richards *et al.*, 2011].

Between the Santa Cruz and Matthew Island, a clear Wadati-Benioff zone reveals the existence of the Australian slab down to 250 km, and locally to 350 km [Pascal *et al.*, 1978] (Figures 2 and 4). At the southern end of the New Hebrides subduction, the slab shows two abrupt changes. A first discontinuity is observed around  $20^\circ\text{S}$  where the maximum depth of earthquakes suddenly changes from  $\sim 250$  to  $\sim 150$  km, likely reflecting a sudden shortening of the slab [Pascal *et al.*, 1978; Coudert *et al.*, 1981; Louat, 1982] (Figures 2 and 4). At around  $172^\circ\text{E}$ , a second discontinuity is marked by a drastic sharp drop in the number of recorded earthquakes [Louat, 1982; Monzier *et al.*, 1984; Maillet *et al.*, 1989; Richards *et al.*, 2011; Lister *et al.*, 2012]. A decrease in statistical significance due to the small number of earthquakes complicates the interpretation of the second discontinuity, resulting in poorer constraints on slab geometry.

### 3. Results

#### 3.1. Seafloor Morphology From Multibeam Data

Multibeam data (Figures 5–8) show a N-S spreading system as far south as  $22^\circ\text{S}$ , already suspected by Tanahashi *et al.* [1994]. The V shape of the southern extremity of this system suggests that it has been propagating toward the South. We have named this feature the Eissen Spreading Centre (ESC) and the basin

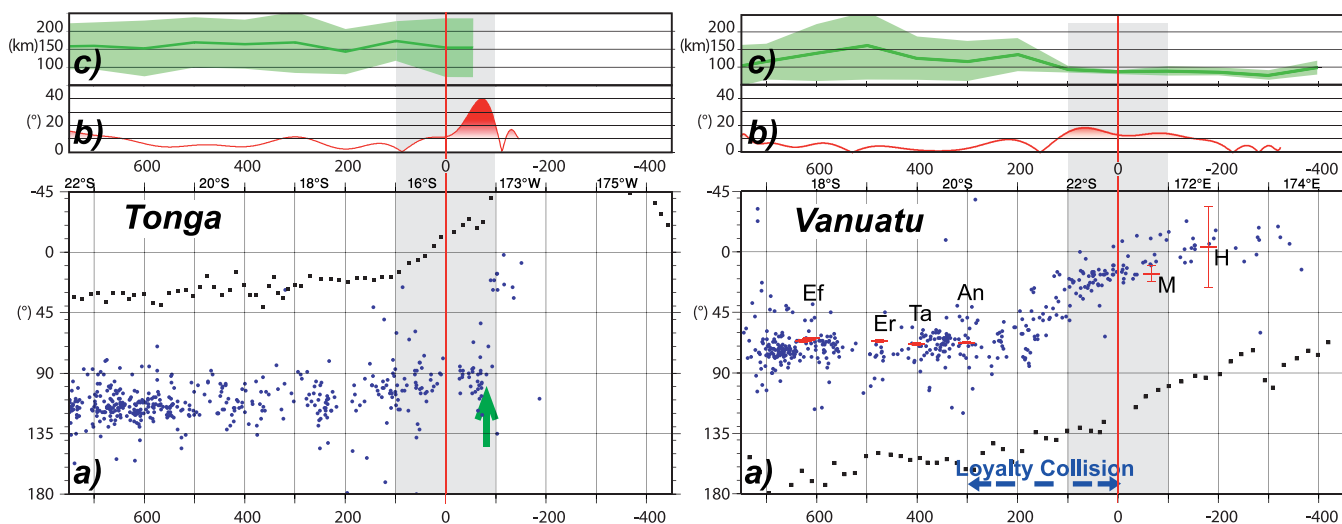


**Figure 3.** (a) Evolution of the azimuth of slip vectors in degrees (blue dots) along the (left) Tonga and (right) New Hebrides subduction zones. The black dots correspond to the strike of the trench. The horizontal axis corresponds to distance along the subduction (km) from the subduction direction inflection point (red stars in Figures 1 and 2). Vertical axis corresponds to orientation (°) relative to the North. Note, for the Tonga subduction, the sharp change of azimuth around  $-100$  km (green arrow) is in marked contrast to the much more continuous change along the New Hebrides subduction. GPS measurements indicating the directions of motion relative to the Australian plate [Calmant *et al.*, 2003] are marked in red, with their error bars, at Efate (Ef), Tanna (Ta), Erromango (Er), Matthew (M), and Hunter (H) islands. (b) The red curve corresponds to difference in degrees between the observed slip vectors and their expected direction (perpendicular to the trench). In New Hebrides, this difference stays below  $20^\circ$ , with the slip vectors direction changing together with the direction of subduction, while in Tonga it reaches  $40^\circ$ , the slip vectors being locally very oblique to the subduction. (c) Position of the arc relative to the trench with distances in km. The 2300 m isobaths has been chosen arbitrarily as a good envelope of the morphological expression of the volcanic arc (green area); its median is marked as a thick green line. In Tonga, even if numerous major arc-like volcanoes exist along the northernmost boundary of the Lau Basin, the high continuous ridge associated to the arc stops abruptly at the bend while it only narrows in New Hebrides. See text for more discussions. Details on the construction of this figure can be found as supplementary information (supporting information S1).

around the spreading center the Eissen Spreading System. From  $174^\circ\text{E}$  to  $172.8^\circ\text{E}$ , the southern extremity of the spreading system is relayed by the *Monzier Rift*, an elongated  $60\text{ km} \times 12\text{ km}$  valley striking  $\text{N}65^\circ$ . The steep shoulders on the sides of the valley, and the numerous individual volcanic edifices in its center suggest the valley opened as a rift. At its southwestern edge, the *Monzier Rift* narrows progressively to a straight graben then finally to a linear incision, interpreted as a strike-slip fault. This fault ends abruptly at Hunter Island (Figure 5). Three areas are therefore distinguished: the Eissen N-S spreading system, the  $\text{N}65^\circ$  *Monzier Rift* valley, and the western strike-slip fault and volcanic domes.

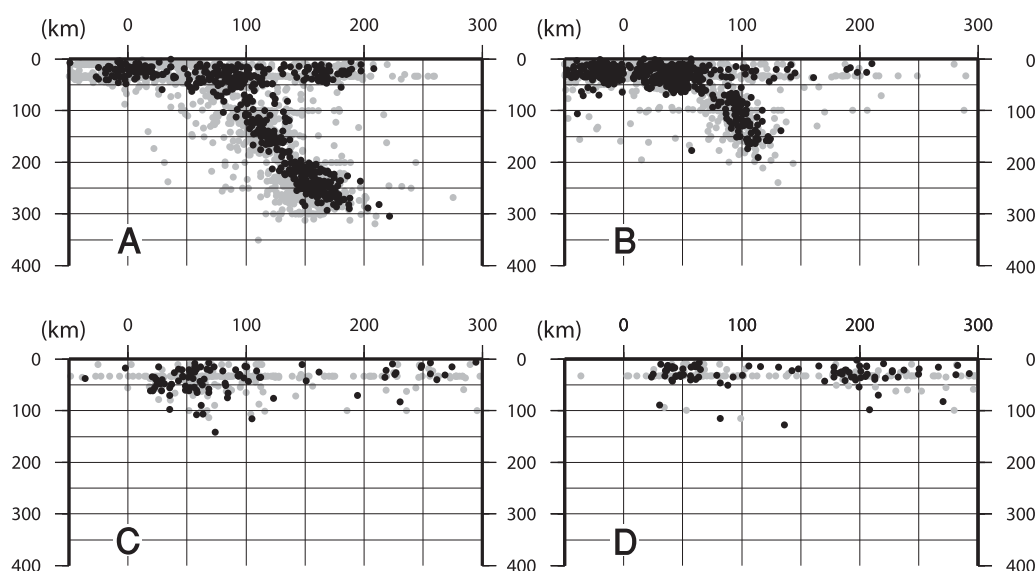


**Figure 4.** Seismic cross sections along four profiles perpendicular to the trench (localized in Figure 2). The shortening of the slab from A to C is achieved abruptly, by steps. See text for more explanation. Hypocenters within 150 km of each profile are projected orthogonal to the trench. All distance units are in km (note the vertical exaggeration). Zero on horizontal axis corresponds to the intersection with the trench. Gray circles are hypocenters recorded in the USGS catalog. Black circles correspond to hypocenters in the ISC EHB bulletin.



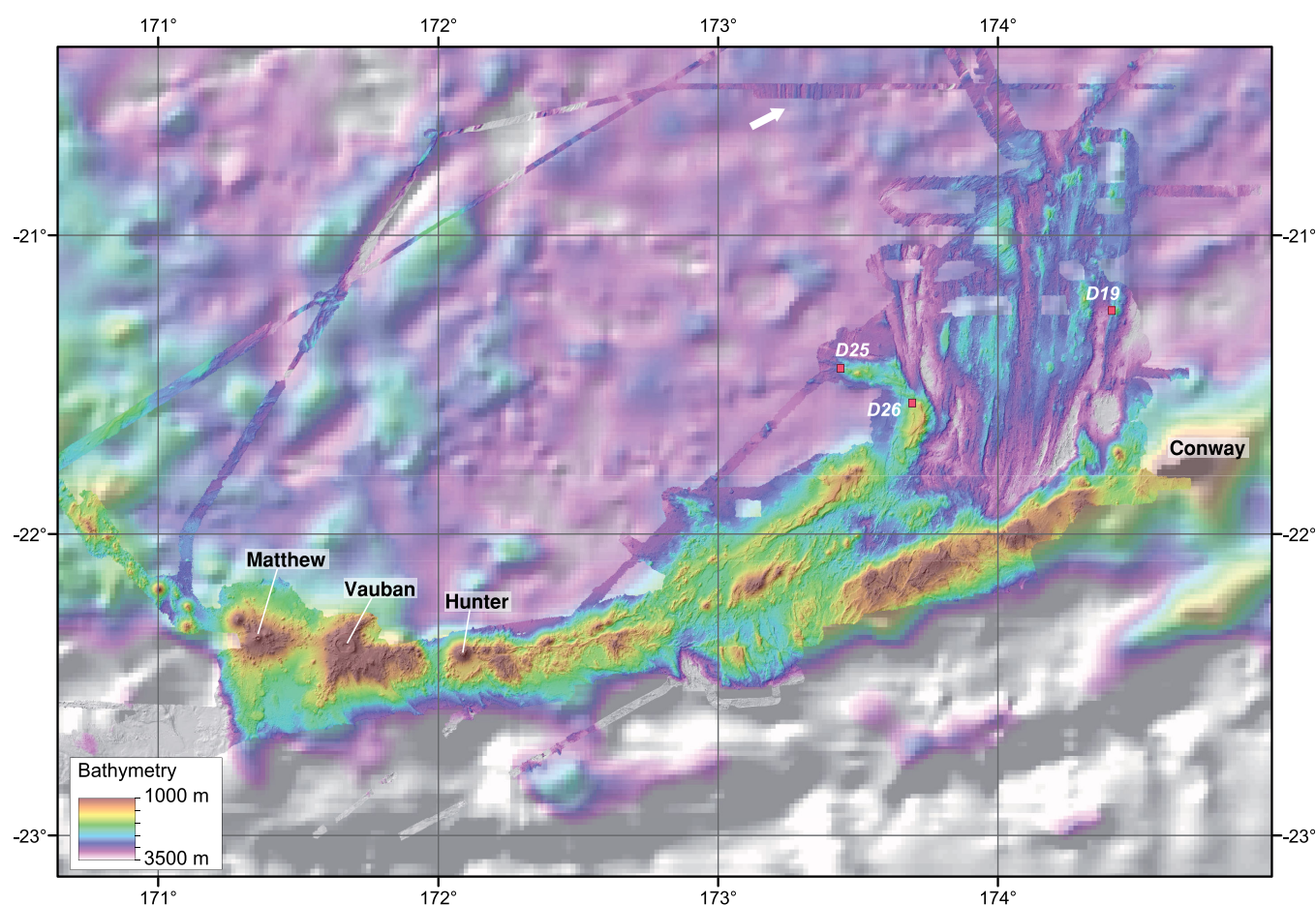


**Figure 5.** Bathymetric map of the surveyed area illuminated from the N. Multibeam data are from R/V Southern Surveyor (SS04/10, SS06/08, SS09/02, and SS09/03 Research Voyages) and satellite data [Smith and Sandwell, 1997]. Red squares correspond to dredged samples discussed in the text and whose geochemical analysis is given as supporting information Table S1. The white arrow shows to the southernmost part of the Central Spreading Ridge mapped by multibeam bathymetry.

### 3.2. The N-S Eissen Spreading Centre

The Eissen spreading system is characterized by abyssal hills elongated predominantly in a northerly to north-north easterly direction with a central axial topographic depression around 3000 m deep, 3 km wide and with a strong backscatter signal (Figures 6 and 9).

South of 21°30'S, the mapped southern termination of the basin is V-shaped suggesting the spreading center propagated 30 km southward until 22°S. The propagator edge and corners are very well marked by abyssal hills abutting against an abrupt escarpment.

Toward the southwest, a smoother change of bathymetry from around 3000 to 2500 m marks the transition between the Eissen spreading system and the Monzier Rift. At this transition, the abyssal hills have clear sigmoidal shapes.

The structure at the northern end of ESC is more complicated. On the eastern side of the spreading axis, the linear axis-parallel features continue as far north as at least 20.65°S, whereas on the western side they terminate, around 21°S, against a shallower block adjacent to the axis, which has E-W topographic lineations. Approximately 30 km west of the axis, the linear abyssal hills curve progressively eastward around the shallower block, changing to the E-W direction north of it. The axis itself abruptly ends against this E-W fabric at ~20.8°S.

The presence of the CSR spreading axis at 173.3°E is revealed by an E-W multibeam bathymetric profile at around 20°30'S (Figure 10). However, the lack of multibeam data between the southern end of the CSR and the northern end of the ESC does not allow us to characterize the connection between these two spreading centers.

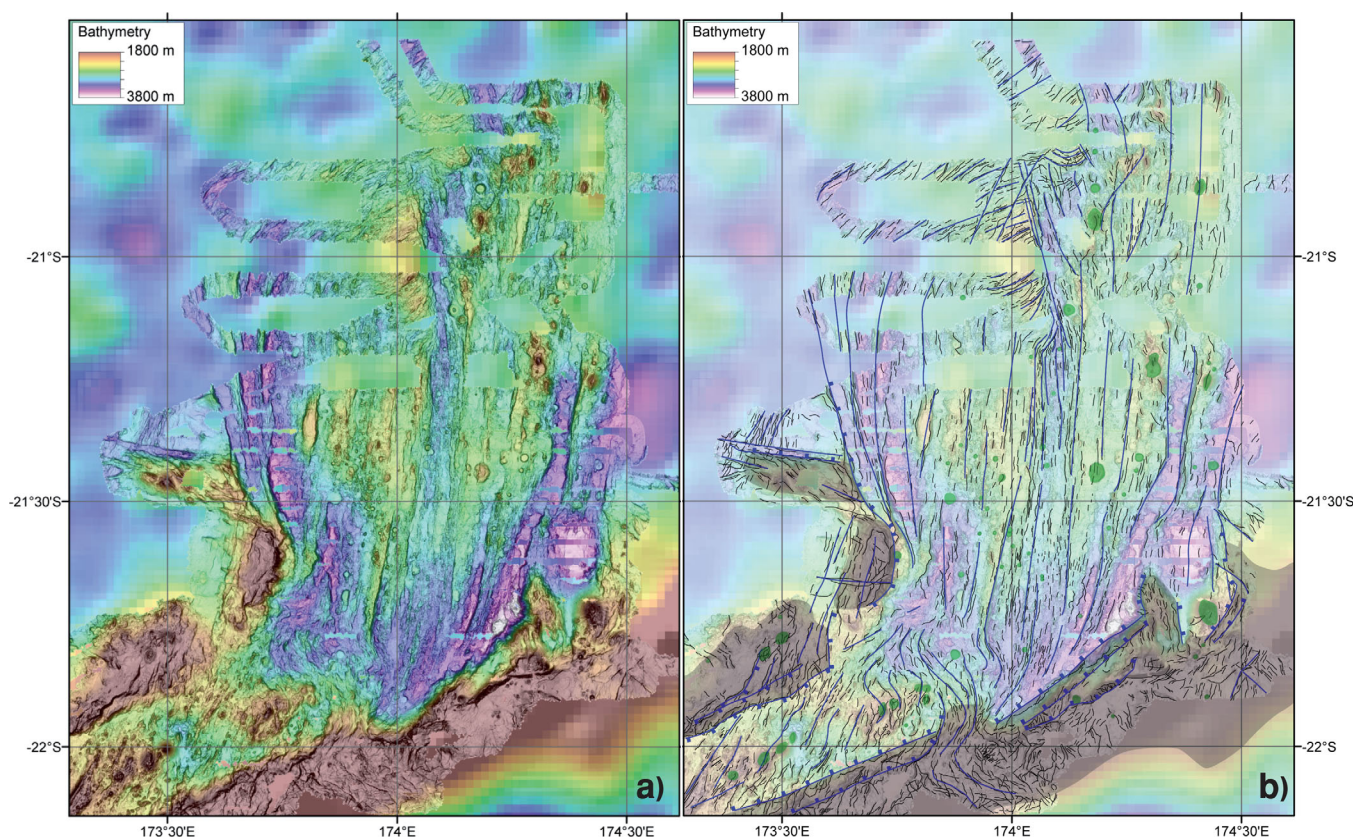


**Figure 6.** The N-S Eissen Spreading Centre. (a) Bathymetry. (b) Interpretation with major lineaments (black lines) and volcanic domes (green).

Additionally, an ESE-WNW escarpment, orthogonal to the current spreading axis and abyssal hills, is observed on the western side of the ESC at  $\sim 21.4^{\circ}\text{S}$ ,  $173.5^{\circ}\text{E}$ . Its origin is discussed later in this paper.

### 3.3. The Monzier Rift Valley and Shoulders

At its southern end, the Eissen spreading system described above is connected to a  $\text{N}65^{\circ}$  elongated perched valley, 60 km long and 15 km wide (Figure 7). The valley floor is characterized by a strong backscatter signal compared to its sides.

Numerous volcanic seamounts and ridges emerge from the relatively flat valley bottom (2200–2400 m depth) 500–1500 m below the rift shoulders. These volcanic ridges and seamounts have various dimensions and most of them are elongated in a NNE direction ( $030^{\circ}$ ), arranged en-echelon and centered along the axis of the valley.

The valley is bounded by a high and steep escarpment, mostly composed of two to three steps, oriented parallel to the valley axis. Toward the southwest, the height of escarpments on both sides of the rift valley progressively decreases as a result of the shallowing of the valley. The volcanic edifices in this area are larger, with some rising above the shoulders of the rift.

The northern shoulders of the rift consists in a relatively shallow and flat plateau ( $\sim 1200$  mbsl), which deepens toward the southwest (Figure 7a). Toward the northwest, the plateau deepens gradually to a 3000 m deep abyssal plain.

The southern shoulder deepens rapidly southward down to a trough about 4000 m deep. The exact topography between the southern slopes of the Hunter Ridge and the New Hebrides Trench in this area is not known. Based on the satellite bathymetry, this trough is separated from the main subduction trench by a ridge shallower than 3000 m (Figure 10). The tectonic relationship between the Monzier Rift and this ridge is unclear; however, it appears that the deep graben aligned along  $\text{N}150^{\circ}$ , which cuts through the southern shoulder of the Monzier Rift at  $\sim 172.8^{\circ}\text{E}$  (Figure 7), is topographically connected with the main subduction trench (Figure 10).



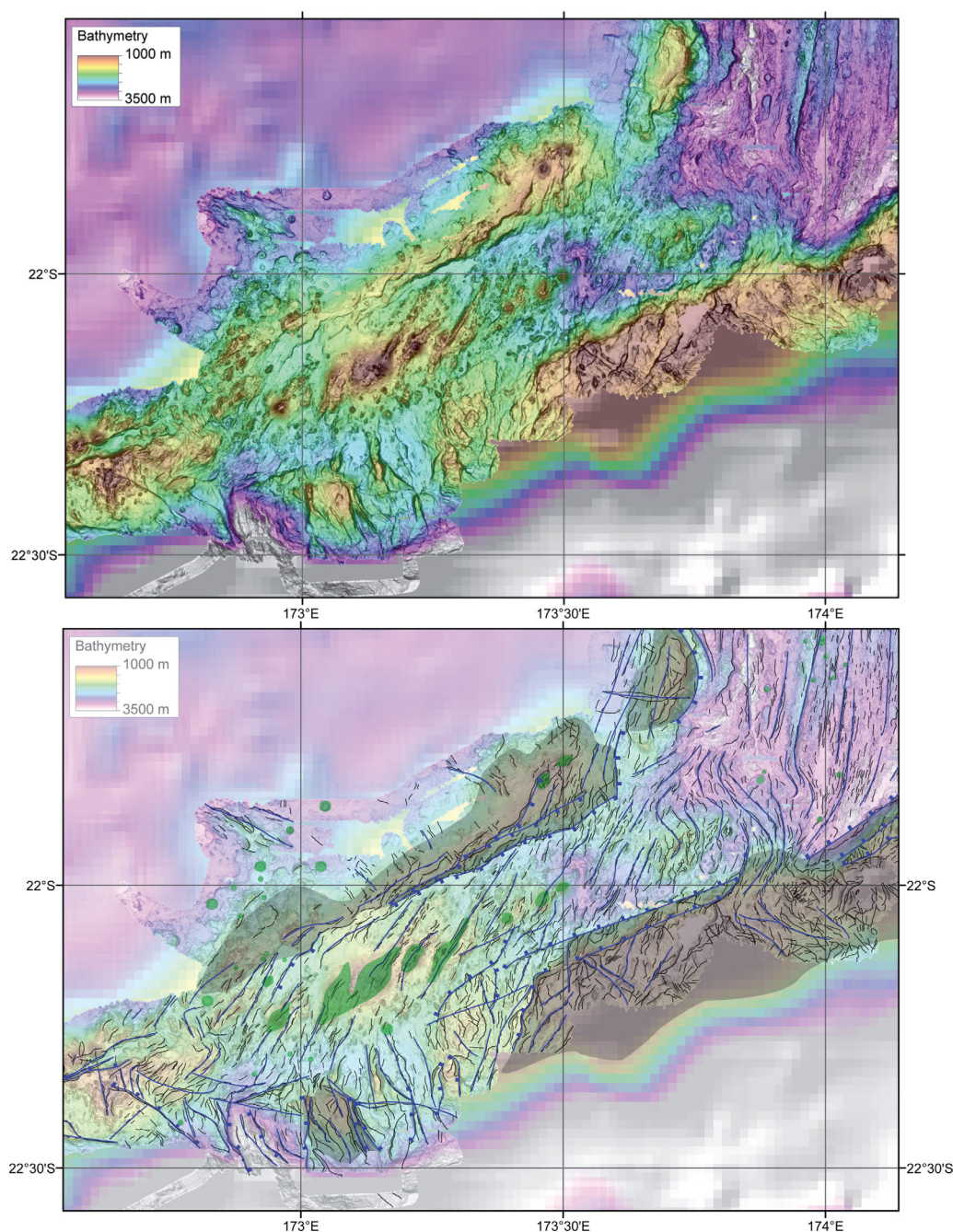


**Figure 7.** The Monzier Rift valley and shoulders. (a) Bathymetry. (b) Interpretation with major lineaments (black lines) and volcanic domes (green).

### 3.4. The Western Transform Fault and Volcanic Domes

At its southwest end, the Monzier Rift is replaced by a lumpy ridge, about 15 km wide, marked in its center by long and extremely thin rib-like ridges that very often constitute the apex of the wider ridge, and by a series of narrow and deep grabens, both aligned in a N75° to N90° directions (Figure 8). This ridge terminates by abutting against the eastern flank of Hunter Island.

The Hunter, Vauban, and Matthew volcanoes are aligned in a N95° direction (Figure 8), in line with the ridge to the East of the Hunter Island and parallel to the subduction trench.

A network of N120° to N160° faults cuts the southern flanks of the ridge and the three volcanoes, however, these faults do not appear to exist on the northern slope.

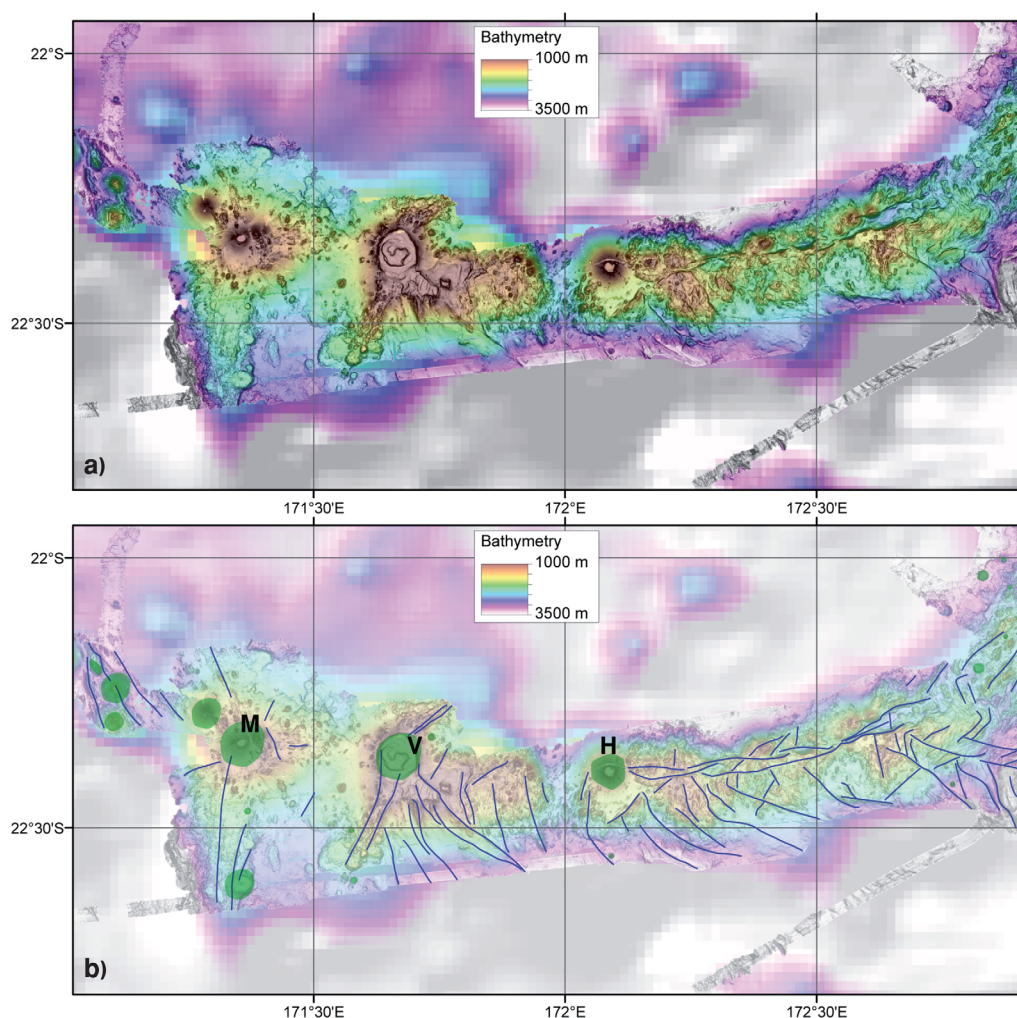


**Figure 8.** The western transform fault and volcanic domes. (a) Bathymetry. (b) Interpretation with major lineaments (black lines) and volcanic domes (green). H, Hunter Island; M, Matthew Island; V, Vauban Seamount.

### 3.5. Magnetic Anomalies of the N-S Spreading System

Total magnetic intensity data were acquired across the ESC during the Southern Surveyor expeditions and combined with data from *Collot et al.* [2009] (Figure 9). Magnetic anomalies were derived by subtraction of the IGRF 2011 global field from the recorded field. The systematic variations between positive anomalies (red) and negative anomalies (blue) confirm the interpretation of this region as an active spreading center.

A synthetic profile has been calculated using a two-dimensional block model assuming opening in a  $N95^\circ$  direction with a half rate of  $17.5 \text{ mm yr}^{-1}$  and the geomagnetic polarity time scale from *Ogg* [2012]. This synthetic profile is drawn in Figure 9 for reference. The identification of the Brunhes-Matuyama and C2n anomalies (Figure 9) further allowed us to propose a full opening rate of  $3.5 \text{ cm yr}^{-1}$  for the 0–1.78 Ma period. The magnetic anomalies also suggest that, south of  $21.5^\circ\text{S}$ , the oceanic crust accreted along the ESC is younger than 1.78 Ma. Finally, south of  $21.5^\circ\text{S}$ , the V-shape of the seafloor morphology and magnetic lineations, and the age of the latter, suggest the ESC propagated southward since 1.78 Ma.

### 3.6. Structural Interpretation

The new data set confirms and details the connection of the ESC with the Hunter Ridge as proposed by *Maillet et al.* [1989]. From  $174^\circ\text{E}$  extension is progressively shifted south-westward along the Monzier Rift (wide gray area in Figure 10), which cuts the Hunter Ridge. Micro segments along the Rift axis form a series of NE-SW elongated seamounts aligned en-echelon in the center of the Rift.



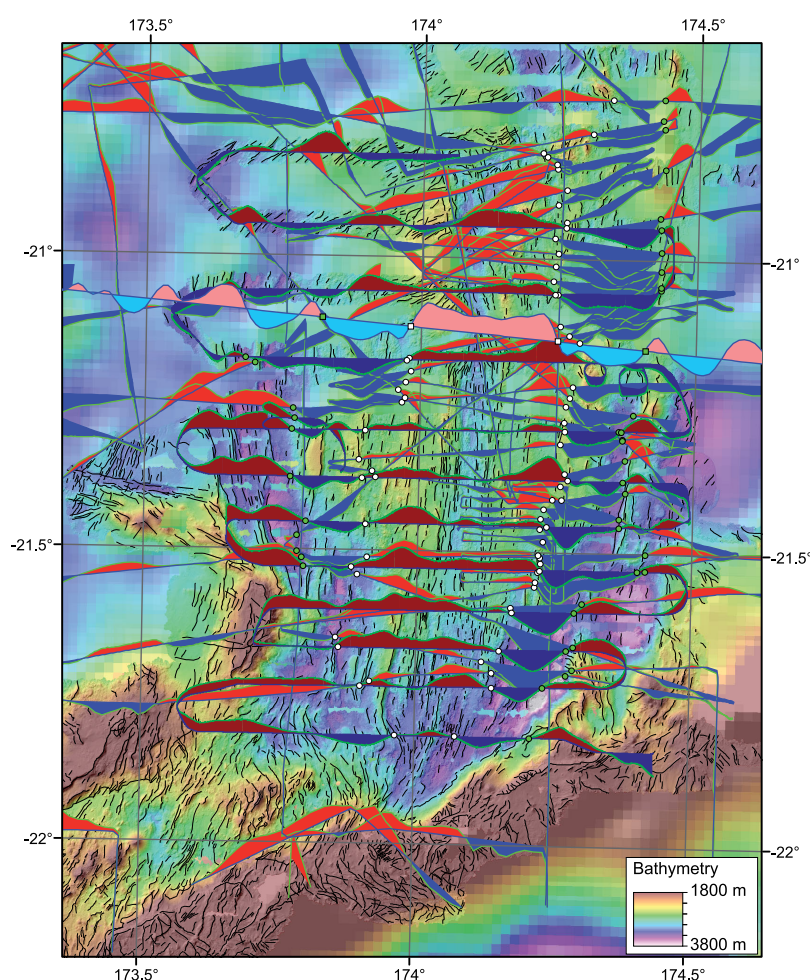


**Figure 9.** Magnetic anomalies along ship track superposed on bathymetry (UTM59S projection). Magnetic data in dark blue and red are from this study, other data are from *Collot et al.* [2009]. A synthetic magnetic anomaly profile (pink and cyan), calculated using a two-dimensional block model and assuming a full opening rate of  $3.5 \text{ cm yr}^{-1}$  and an opening direction  $\text{N}95^\circ$ , has been superimposed for reference on the figure. We picked the Brunhes-Matuyama limit (C1r.1r, white dots,  $\sim 0.781 \text{ Ma}$ ) and the young edge of anomaly 2 (C2n, green dots,  $\sim 1.778 \text{ Ma}$ ).

West of  $172.7^\circ\text{E}$ , the deformation localizes on an E-W sinistral strike-slip system that can be followed until the Hunter Island but is not detected further west. This strike-slip system is characterized by an alternation of E-W strike-slip faults and NE-SW pull-apart grabens.

As discussed below, these observations can be explained by a simple model where the observed extension (gray area in Figure 10) corresponds to a single boundary between two microplates diverging in the E-W direction (double-sided red arrows in Figure 10).

## 4. Discussion

### 4.1. Kinematics of the Upper Plate Explains the North-South Convergence at the New Hebrides Subduction Termination

The change of slip vector direction observed along the New Hebrides subduction south of  $22^\circ\text{S}$  cannot be explained by the kinematics of a system constituted by only two rigid plates [*Louat and Pelletier*, 1989]. The distribution of shallow earthquakes within the North Fiji Basin suggests the latter consists of several microplates. *Louat and Pelletier* [1989] explored this hypothesis and proposed a model involving 4–6 microplates within the North Fiji Basin that is consistent with the deformation as deduced from the seismicity. Notably, at the southern termination of the New Hebrides subduction, the relative movement between southern Vanuatu (the “Southern New Hebrides Arc” plate (SNHA) in *Louat and Pelletier* [1989]) and the Matthew and

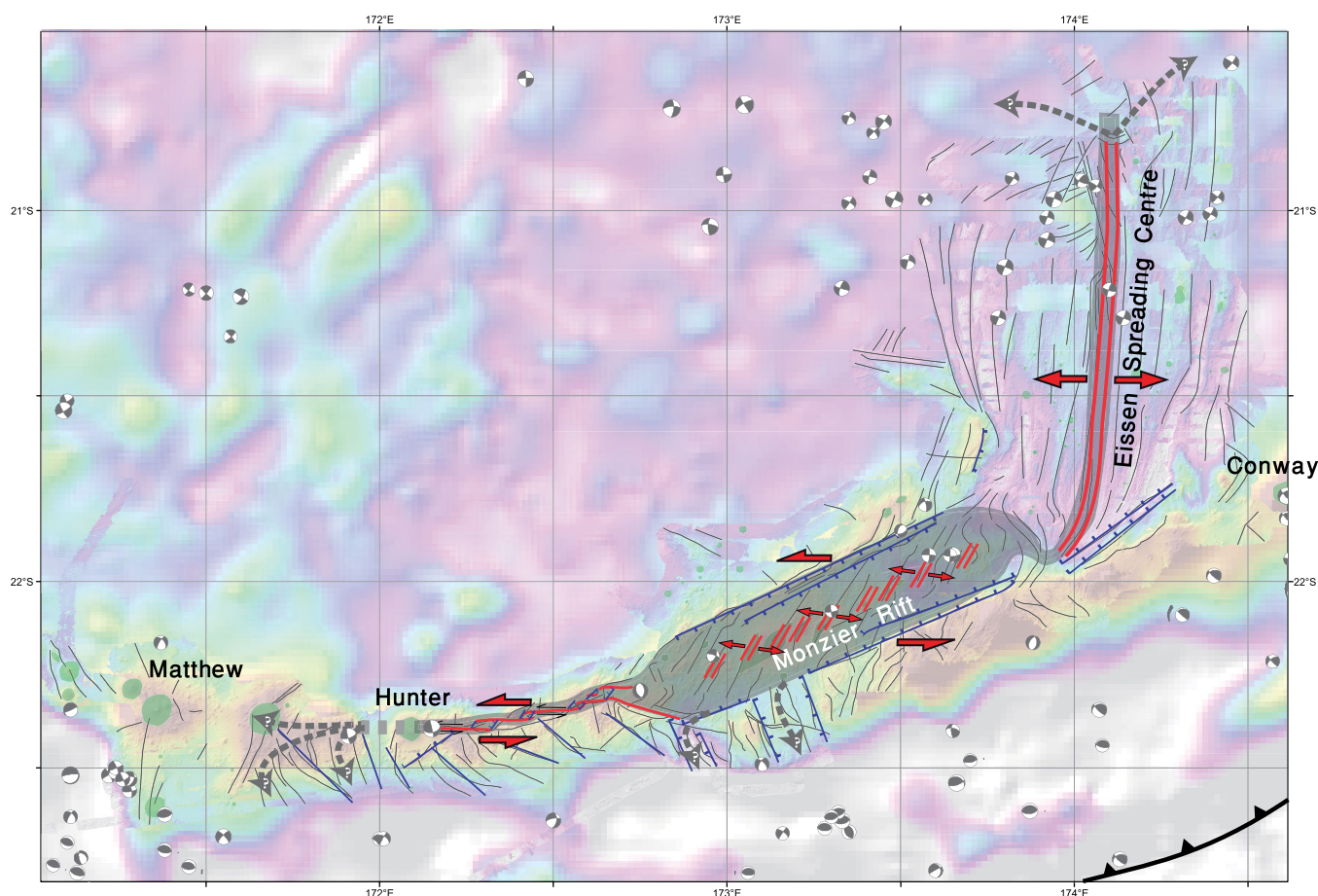


**Figure 10.** Simplified structural map of the surveyed area. The gray surface corresponds to the actively deforming area at a boundary between two microplates whose relative motion is marked by red arrows. Gray dotted arrows schematize our failure to precisely identify where this deforming area connects at the edge of the mapped area, westward beyond Hunter, south of the Monzier Rift and northward beyond 21°S.

Hunter area (the “Southern North Fiji Basin” plate (SNFB) in Louat and Pelletier [1989]) is accommodated by an E-W sinistral strike-slip zone somewhere between these two plates. The relative motion between Aneytum and Matthew Islands, as deduced from GPS measurements, is consistent with this hypothesis [Calmant *et al.*, 2003].

The new geophysical data presented here, as well as more than 15 years of additional earthquakes recorded in the area by the international seismic network, allow us to complement the structural model proposed by Pelletier *et al.* [1998] for the North Fiji Basin (Figure 11). New boundaries (thick and transparent lines in Figure 11), either transform (black lines) or divergent (red lines), have thus been added to their model mainly in the southern part of the basin.

Bathymetry predicted from satellite altimetry [Smith and Sandwell, 1997] combined with earthquakes epicenters and focal mechanisms suggest the southern end of the Central Spreading Ridge continues toward the southwest through an alternation of E-W or ESE-WNW transform faults and NE-SW spreading axis until the subduction at 22°S where the Loyalty Ridge collides with the arc. Even though these new features have as yet not been confirmed by multibeam echosounding, the consistency between earthquakes (epicenters trends (Figure 11) and mechanisms (Figure 2)) and seafloor morphology (Figure 2) gives strong support to our proposed tectonic model.

Central to this model is the prolongation of the CSR toward the southeast along a transform system that connects the CSR to the ESC. This is supported by the occurrence, between these two spreading centers, of numerous strike-slip type earthquakes (Figure 2). However, these earthquakes, their distribution over a wide (~50 km) zone and their focal planes oblique to the spreading axis, do not



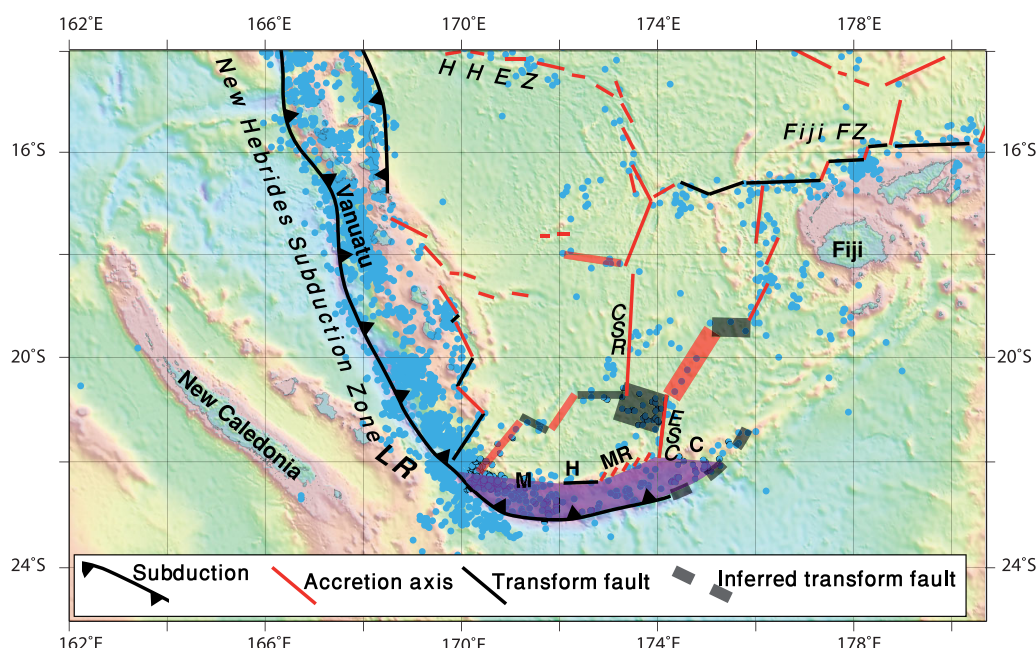


**Figure 11.** Tectonic setting of the North Fiji Basin after Pelletier [1999] and this study. The background is satellite bathymetry [Smith and Sandwell, 1997]. Blue circles are shallow (<50 km) earthquakes from the USGS catalogue. CSR, Central Spreading ridge; Fiji FZ, Fiji Fracture Zone; H, Hunter; HEZ, Hazel Holme Extensional Zone; ESC, Eissen Spreading Centre; M, Matthew; MR, Monzier Rift. New interpretations are drawn as transparent lines. Their thickness is proportional to the uncertainty associated with them (see text for explanations). Because of the absence of geophysical information in the purple area South of Matthew and Hunter islands no new interpretation of this zone has been made. However, the deformation zone we described at the southern end of the N-S accretionary system connects necessarily with the trench somewhere between 170°E and 173°E.

correspond with the sharp E-W dextral transform fault we would expect in this area. Moreover, the strike-slip earthquakes cluster too far south compared to the latitude of the junction between the ESC and the CSR. Unfortunately at present no additional information is available on the seafloor morphology in this area.

South of 22°S (purple area of Figure 11), the situation remains unclear, despite the new data set. In the area covered by the new geophysical data, a narrow deformation zone occurs along the Hunter Ridge and corresponds to a microplate boundary (gray area of Figure 10). This boundary runs from the Eissen Spreading Centre to the Monzier Rift and the transform zone, before abutting against the Hunter Island. But it cannot kinematically just stop. It must somehow connect with another plate boundary; either the subduction to the south or to the west. Clear N-S grabens exist to the south of the rift valley around 173°E (Figure 10). N-S or NW-SE fracturing and earthquakes suggest a series of similar NNW-SSE grabens could exist from 174°E (South of the Eissen Spreading Centre) to 171.5°E (South of Matthew Island). This graben network could provide the expected kinematic link toward the subduction, either forming a diffuse boundary with several of these grabens deforming together, or one of them (i.e., at the longitude of the Hunter Island or slightly westward of it) serving as a single boundary. The grabens system has not been entirely surveyed and the continuity of these grabens toward the subduction front cannot be established at this stage. Another possibility is that this graben system could also be kinematically independent from the microplate boundaries discussed above, and simply be a consequence of arc-parallel extension observed in many arcs, and related to the increase of the curvature of the arc [e.g., Schellart and Lister, 2004].

The absence of data south of 22°S prevents us from proposing a more comprehensive model of the southern termination of subduction. However, the new geophysical data obtained after the work of Pelletier *et al.* [1998] not only confirm the change of slip vector at the southern termination of the subduction but also reveals that this change is progressive along the arc. We can therefore be confident of the existence of secondary boundaries or of diffuse deformation inside the North Fiji Basin, which fragment the upper plate and hence provide kinematic solutions fully consistent with GPS measurements and earthquake slip vectors.

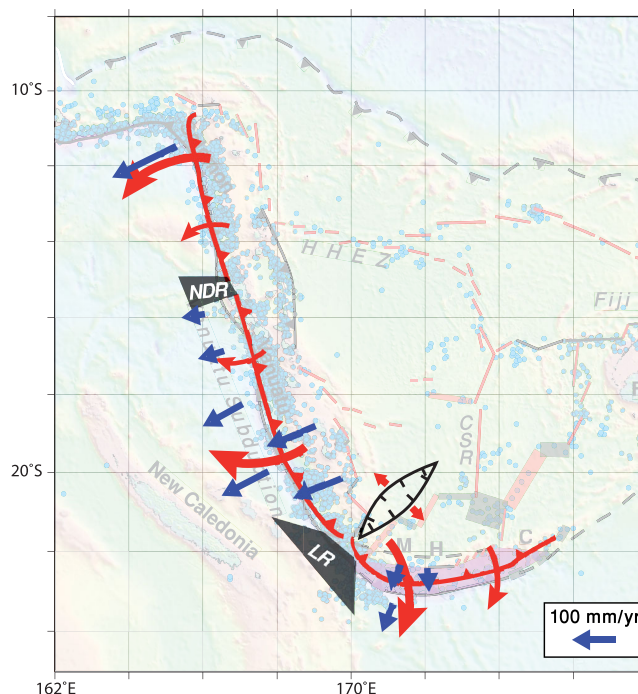


**Figure 12.** Schematic interpretation of the present day situation. Red arrows correspond to schematized motion relative to Australia at subduction. Gray indenters correspond to North D'Entrecasteaux Ridge collision (NDR) and Loyalty Ridge collision (LR). Blue arrows are motion relative to Australia according to estimations of Pelletier *et al.* [1998] and to GPS measurements from Calmant *et al.* [2003], with their scales on bottom right.

the subduction continues on both sides of the indenter (note this is different from the analogue models of Schellart *et al.* [2002]). The mega tension fracture (the accretion axis) accommodates the motion between fragments of the upper plate that move in opposing directions on both sides of the indenter toward the free borders (Figure 12).

The tectonic pattern observed today in front of the Loyalty collision would be an equivalent to the earliest stage of the D'Entrecasteaux Ridge collision [Green and Collot, 1994; Schellart *et al.*, 2002]. This analogy suggests that, in front of the Loyalty collision, backthrusting could occur soon on the back arc side of the arc. But more interestingly it also suggests that, in front of the D'Entrecasteaux Ridge, NE-SW spreading axis and normal faults could have been active at an early stage and such fossil faults could be found NE of Santo Island. The Hazel Holme Extensional Zone, characterized by a high angle compared to the trend of the arc, could have initiated at this early stage of the D'Entrecasteaux Ridge collision.

#### 4.3. How Long did the N-S Convergence at the Southern Termination of the New Hebrides Subduction Last?

An age of 7 Ma has been proposed for the initiation of the N-S subduction along Hunter Ridge [Auzende *et al.*, 1995; Pelletier, 1999]. This is deduced from the inception of N-S accretion along the E-W spreading axis located in the North of the NFB. However, this N-S motion, resulting from the opening along the E-W spreading ridge, corresponds to the relative motion between the Pacific plate and the New-Hebrides plate to the South (Hunter Ridge) and southwest (Vanuatu Arc), while the inferred new subduction margin is involving New Hebrides and Australia, not Pacific. The relevant approach, therefore, is to evaluate the motion between the Hunter ridge and the Australia plate, hence to also take into account the Australia/Pacific relative motion which, globally E-W, very likely results in the Hunter ridge/Australia motion being NE-SW, and therefore still being consistent with a transform margin. Moreover, opening along both the NW-SE and E-W spreading axis can be described by one single rotation pole situated in the NW of the NFB. Hence, the switch, from NW-SE to E-W spreading axis does not imply a change of relative motion along the southern border.

#### 4.2. Speculations About the Causes for Such a Tectonic Setting

The geometry of the fragmentation at the southern margin of the NFB, in particular, the high angle of spreading ridges with respects to the arc, and the age of this deformation, strongly suggest such fragmentation could be a consequence of the collision of the Loyalty Ridge against the New Hebrides Arc as already suggested by Monzier *et al.* [1984, 1989, 1990], Maillet *et al.* [1989], and Monzier [1993] and similarly to what was proposed by Schellart *et al.* [2002] for the D'Entrecasteaux Ridge collision.

The subduction progression is blocked or slowed in front of the Loyalty collision, while convergence proceeds elsewhere. From an upper plate perspective, the Loyalty ridge acts like an indenter that progresses toward the NE [Monzier *et al.*, 1990]. Opening of the speculated NE-SW spreading axis (Figure 11) could be seen as a mega tension gash just in front of the indenter. In this model,

Moreover, the lack of deep earthquakes east of 171°E along the southern termination of the New Hebrides subduction zone confirms that northward subduction beneath that part of the arc began only recently.

Louat [1982] proposed an age of ca. 2 Ma for the subduction south of 20°S by using the length of the Wadati-Benioff zone (160 km from 20°S to 172°E) and an estimated convergence rate of 10 cm/yr. Both a length and a rate have been confirmed since the time of this publication [Louat and Pelletier, 1989; Calmant *et al.*, 1995, 2000, 2003; Pelletier *et al.*, 1998].

Finally, speculations about a possible cause and effect relationship between the Loyalty Ridge collision, the Southward propagation of the Eissen Spreading Centre beyond 21.5°S and the N-S convergence initiation led us to consider these three events could be more or less synchronous. In that case, the ~1.78 Ma age of spreading associated to the Eissen Spreading Centre (Figure 9) could also be the age of the start of the N-S convergence.

Before 1.78 Ma, the New Hebrides subduction zone terminated around 22°S through a transition to a sinistral transform fault (Figure 13). The N-S subduction was very likely initiated along that transform fault.

#### 4.4. Does an Australian Slab Exist East of Hunter Island?

The existence of a slab, with earthquake hypocenters deeper than 100 km along the Wadati-Benioff seismic plane, is attested up to 172°E, the longitude of Hunter Island (Figures 2 and 4). However, the New Hebrides subduction is associated with a deep trench and active volcanism beyond 172°E, at least up to 174.5°E. Moreover, the arc-trench distance does not change much in this area, with the arc curving in parallel with the trench (Figure 3). It is worth noting that, in contrast, the Northern Tonga arc does not curve in parallel with the trench, active volcanoes suddenly get much closer to the trench north of 16°S, which corresponds with the subduction-to-transform-transition. Following a general interpretation of the relationship between the depth of the slab and the location of the volcanic arc [Tatsumi and Eggins, 1995], we are inclined to interpret this stability of the arc-trench distance as an indication of the existence of a slab without major dip change until ~175°E. But this assumption is valid only if the magmas come from a similar source and melting depth.

A further confirmation of the continuation of subduction up to ~175°E is the existence of active volcanic centers producing typical subduction-related lavas [Danyushevsky *et al.*, 2006]. Today, we have no geophysical information about the presence of a slab deeper than 100 km east of Hunter Island (Figures 2 and 4). This is not in conflict with the age proposed above, where we speculated that the beginning of the N-S convergence coincided with the initial opening of the ESC at 1.78 Ma. Such an age, associated with a convergence rate of 50 mm/an (60 mm/an according to Pelletier *et al.* [1998]; 48 mm/an according to Calmant *et al.* [2003]), corresponding to half the rate characterizing the subduction along the main New Hebrides Arc further northwest, would give a total amount of convergence of ~90 km and therefore a similar length for a slab produced from this process. Convergence of 90 km could drive the oceanic crust deep enough to trigger partial melting [Gill, 1981; Tatsumi and Eggins, 1995].

This hypothesis is supported by hypocenters recorded in the USGS catalog (<http://earthquake.usgs.gov/earthquakes/search/>) and in the ISC EHB bulletin [Engdahl *et al.*, 1998] (<http://www.isc.ac.uk>). In these two databases, intermediate earthquakes hypocenters as deep as 100 km exist east of 172°E, up to 175°E. It is worth noting that no such deep earthquake is recorded in the CMT Global Project catalog [Ekström *et al.*, 2012] (<http://www.globalcmt.org/>) to the east of Matthew Island, meaning that no major earthquake (magnitude >5.0) deeper than 50 km has been recorded in this area.

#### 4.5. Tectonic Nibbling of the Hunter Ridge

The kinematic situation in the study area (Figure 10) is an E-W divergence between two microplates. This E-W divergence is expressed either as E-W sinistral strike-slip movement, or as extensional rifting of a pre-existing arc (the Monzier Rift) or as crustal accretion localized along a spreading ridge (the Eissen Spreading Centre). If the current process continues, extension in the rifted area will rupture the crust and give way to crustal accretion along a new spreading axis. Such an evolution from rifting to spreading has certainly already happened recently in the Southern part of the Eissen Spreading Centre, south of 21.5°S. Here the new accreted oceanic crust, characterized by a classical abyssal hills texture and by seabed deeper than 2500 m, is bordered by shoulders of crust, shallower than 1500 m and showing a distinct texture

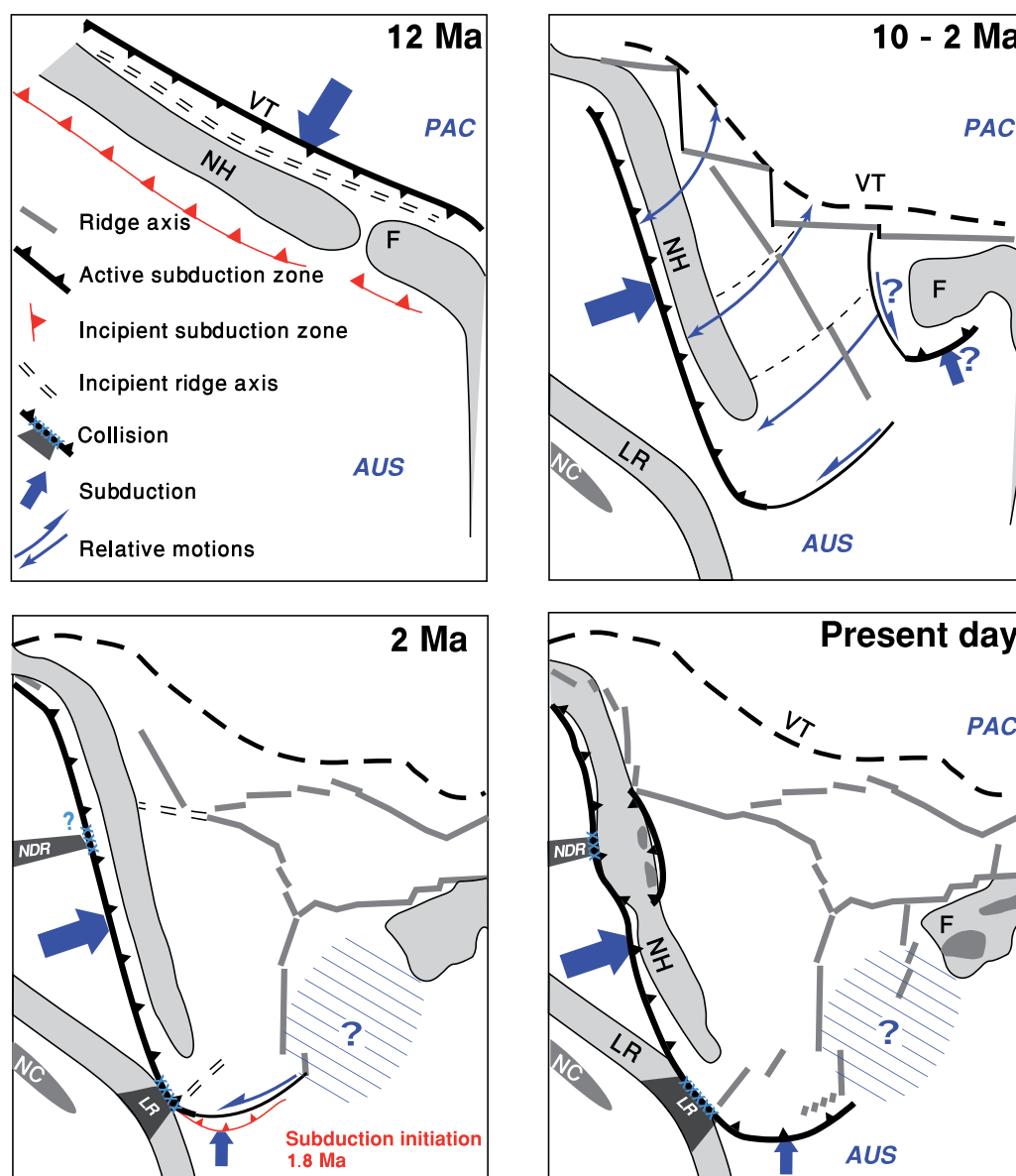


**Figure 13.** Geodynamic evolution of the North Fiji Basin, modified after *Auzende et al. [1995]* and *Pelletier [1999]*. AUS, Australia plate; F, Fiji; LR, Loyalty ridge; NC, New Caledonia; NH, New Hebrides; PAC, Pacific plate; VT, Vitiaz Trench. Note that the relative motion between the New Hebrides and Australia plates, results along the southern margin of the NFB in a sinistral transform fault during the entire 10–2 Ma period.

characterized by a less negative Bouguer anomaly, which clearly formerly belonged to the Hunter Ridge. This suggests that the Eissen Spreading Centre has started as a rift.

We suggest that by this process of rifting and subsequent spreading, pieces are progressively peeled off the Hunter Ridge and incorporated into the North Fiji Back-arc Basin. The current process therefore demonstrates tectonic nibbling of the arc by episodic propagation of the back-arc extension into the arc. Thereby arc pieces isolated by such a mechanism could potentially be found anywhere in the NFB, separated from the main arc by back-arc crust that accreted in between the arc and the isolated crustal fragments.

Such isolated arc pieces should conserve some geophysical characteristics of their arc origin like crustal thickness and density, and should therefore be technically detectable even if embedded within back-arc oceanic back-arc crust. Similarly, they should conserve geochemical characteristics of their arc origin, potentially modified by magmatic products during the rifting process.



Geophysical characteristics of potential isolated arc pieces would be shallow depth (<2000 m below sea level) and lower Bouguer anomaly compared to the surrounding back-arc crust. Several areas with these characteristics are observed in the study area, some of which have been dredged. Dredge sites SS10/2004-D26 and SS10/2004D25 (around 173.5°E, 21.5°S, Figure 5, see supporting information Table S1) are characterized by lavas with typical subduction signature (low-TiO<sub>2</sub> island arc tholeiites), confirming that these two blocks are stranded arc fragments. Note also that the structural fabric of these blocks is orthogonal to the current spreading axis and abyssal hills.

Other small bathymetric highs or seamounts, have some geophysical potential to be similar rifted blocks of arc crust. One of them (SS08/2006-D19, around, 174.5°E, 21.3°S, Figure 5 see supporting information Table S1) was dredged and provided samples with arc-type geochemical characteristics (low-SiO<sub>2</sub> adakites).

Finally, the process of rifting and nibbling has the potential to deconstruct an arc after or during its genesis above subduction.

## 5. Conclusion

New geophysical data from the Hunter Ridge confirm the presence of a back-arc basin spreading ridge named here the Eissen Spreading Centre that extends from 20°S to 22°S, where extension veers to the SW into the Monzier Rift. The Monzier Rift is characterized by sinistral transtension to around 172.7°E where the plate boundary becomes an E-W left-lateral strike-slip zone. A lack of information outside the surveyed area prevents a thorough understanding of where and how this boundary connects with the main New Hebrides subduction zone.

Despite the lack of details, these new plate boundaries are able to explain the overall kinematics of the southern part of the New Hebrides subduction zone. Easterly motion of the southern margin of the North Fiji Basin relative to the main New Hebrides arc is consistent with the southward motion of this Southern margin of the NFB relative to the Australian plate. This southward motion explains the N-S convergence along the subduction in the Matthew and Hunter area, evidenced both by GPS measurements and earthquakes focal mechanisms.

We further suggest that the deformation of the southern margin of the North Fiji Basin, the initiation of the N-S subduction around Matthew and Hunter and the Loyalty collision, is linked. As a consequence of the collision of the Loyalty Ridge against the New Hebrides Arc, the subduction is blocked, or slowed, around the site of the collision, while the convergence keeps going elsewhere. The Loyalty collision progresses like an indenter causing the formation of new spreading centers in the overriding plate in front of the indenter, to accommodate continuing subduction on both sides of the indenter.

We deduced an age of 1.78 Ma for the Eissen Spreading Centre from magnetic anomalies. If these processes are linked, this age would correspond to the Loyalty collision and to the initiation of the N-S subduction in the Matthew and Hunter area, all consistent with the shallow nature of the slab east of 171°E.

Finally, the Monzier Rift corresponds to an incursion of back-arc basin extension into a preexisting arc lithosphere. There, rifting followed by spreading will progressively peel a piece off the arc and isolate it into the back-arc basin crust. The exceptional compositional diversity of the magmatic rocks dredged in this area is explained by this incursion of rifting inside an arc lithosphere above an active subduction.

## References

- Auzende, J.-M., J.-P. Eissen, Y. Lafoy, P. Gente, and J. L. Charlou (1988), Seafloor spreading in the North Fiji Basin (southwest Pacific), *Tectonophysics*, **146**, 317–351.
- Auzende, J. M., B. Pelletier, and J. P. Eissen (1995), The North Fiji Basin: Geology, structure and geodynamic evolution, in *Back-Arc Basins: Tectonics and Magmatism*, edited by B. Taylor, chap. 4, pp. 139–175, Plenum, N. Y.
- Brudzinski, M., and W. Chen (2003), A petrologic anomaly accompanying outboard earthquakes beneath Fiji-Tonga: Corresponding evidence from broadband P and S waveforms, *J. Geophys. Res.*, **108**(B6), 2299, doi:10.1029/2002JB002012.
- Calmant, S., P. Lebellegard, F. Taylor, M. Bevis, D. Maillard, J. Recy, and J. Bonneau (1995), Geodetic measurements of convergence across the New Hebrides subduction zone, *Geophys. Res. Lett.*, **22**, 2573–2576.
- Calmant, S., B. Pelletier, R. Pillet, M. Regnier, P. Lebellegard, D. Maillard, F. Taylor, M. Bevis, and J. Recy (1997), Interseismic and coseismic motions in GPS series related to the Ms 7.3 July, 13 (1994), Malekula earthquake, Central New Hebrides Subduction Zone, *Geophys. Res. Lett.*, **24**, 3077–3080.

## Acknowledgments

This research was supported by the Australian Marine National Facility through funding to three research voyages of the R/V Southern Surveyor (SS10/2004, SS08/2006, and SS03/2009; L. Danyushevsky Chief Scientist), and by the Australian Research Council through funding to CODES, the ARC Centre of Excellence in Ore Deposits. We would like to thank the crew of Southern Surveyor and members of the science party for their support during the voyages. Bathymetry data based on multibeam echo sounding systems and acquired during the three surveys can be requested to Australia's National Science Agency CSIRO <http://www.cmar.csiro.au/data/gsm/>. M.P., J.C., and M.F. acknowledge financial support provided by the Marine Geosciences Agreement between the Government of New Caledonia and Ifremer. We also acknowledge the financial support from the ZoNéCo research program of the ADECAL Technopole, notably for supporting a travel between Nouméa and Hobart. Formal reviews by Richard Arculus and two anonymous reviewers, and editorial handling by Janne Blichert-Toft have significantly improved this paper. Most figures were drafted using GMT software [Wessel and Smith, 1998].

- Calmant, S., J. J. Valette, J. F. Cretaux, and L. Soudarin (2000), Tectonic plate motion and co-seismic steps surveyed by DORIS field beacons: The New-Hebrides experiment, *J. Geod.*, **74**, 512–518.
- Calmant, S., B. Pelletier, P. Lebellegard, M. Bevis, F. W. Taylor, and D. A. Phillips (2003), New insights on the tectonics along the New Hebrides subduction zone based on GPS results, *J. Geophys. Res.*, **108**(B6), 2319, doi:10.1029/2001JB000644.
- Cole, R. B., and B. W. Stewart (2009), Continental margin volcanism at sites of spreading ridge subduction: Examples from southern Alaska and western California, *Tectonophysics*, **464**, 118–136, doi:10.1016/j.tecto.2007.12.005.
- Collot, J., R. Herzer, Y. Lafoy, and L. Géli (2009), Mesozoic history of the Fairway-Aotea Basin: Implications for the early stages of Gondwana fragmentation, *Geochem. Geophys. Geosyst.*, **10**, Q12019, doi:10.1029/2009GC002612.
- Coudert, E., B. L. Isacks, M. Barazangi, R. Louat, R. Cardwell, A. Chen, J. Dubois, G. Latham, and B. Pontoise (1981), Spatial distribution and mechanisms of earthquakes in the southern New Hebrides arc from a temporary land and ocean bottom seismic network and from worldwide observations, *J. Geophys. Res.*, **86**, 5905–5925.
- Danyushevsky, L. V., A. J. Crawford, R. L. Leslie, S. Tetroeva, and T. J. Falloon (2006), Subduction-related magmatism along the southeast margin of the North Fiji back-arc basin, *Geochem. Cosmochim. Acta*, **69**(10), A633.
- Danyushevsky, L. V., T. J. Falloon, A. J. Crawford, A. T. Sofia, R. L. Leslie, and A. Verbeeten (2008), High-Mg adakites from Kadavu Island Group, Fiji, southwest Pacific: Evidence for the mantle origin of adakite parental melts, *Geology*, **36**(6), 499–502, doi:10.1130/G24349A.1.
- DeMets, C., R. G. Gordon, and D. F. Argus (2010), Geologically current plate motions, *Geophys. J. Int.*, **181**(1), 1–80, doi:10.1111/j.1365-246X.2009.04491.x.
- Durance, P. M. J., M. A. Jadamec, T. J. Falloon, and I. A. Nicholls (2012), Magmagenesis within the Hunter Ridge Rift Zone resolved from olivine-hosted melt inclusions and geochemical modelling with insights from geodynamic models, *Aust. J. Earth Sci.*, **59**(6), 913–931.
- Ekström, G., M. Nettles, and A. M. Dziewonski (2012), The global CMT project 2004–2010, Centroid-moment tensors for 13,017 earthquakes, *Phys. Earth Planet. Inter.*, **200–201**, 1–9, doi:10.1016/j.pepi.2012.04.002.
- Engdahl, E. R., R. van der Hilst, and R. Buland (1998), Global teleseismic earthquake relocation with improved travel times and procedures for depth determination, *Bull. Seismol. Soc. Am.*, **88**, 722–743.
- Funciello, F., M. Moroni, C. Piromallo, C. Faccenna, A. Cenedese, and H. A. Bui (2006), Mapping mantle flow during retreating subduction: Laboratory models analyzed by feature tracking, *J. Geophys. Res.*, **111**, B03402, doi:10.1029/2005JB003792.
- Greene, H. G., and J.-Y. Collot (1994), Ridge-arc collision; timing and deformation determined by Leg 134 drilling, central New Hebrides island arc, in *Proceedings of the Ocean Drilling Program, Scientific results*, vol. 134, pp. 241–2853, Ocean Drilling Program, College Station, Tex.
- Gill, J. B. (1981), *Orogenic Andesite and Plate Tectonics*, 390 pp., Springer, Berlin.
- Govers, R., and M. J. R. Wortel (2005), Lithosphere tearing at STEP faults: Response to edges of subduction zones, *Earth Planet. Sci. Lett.*, **236**, 505–523.
- Hamburger, M. W., and B. L. Isacks (1987), Deep earthquakes in the southwest Pacific: A tectonic interpretation, *J. Geophys. Res.*, **92**, 13,841–13,854.
- Hole, M. J., G. Rogers, A. D. Saunders, and M. Storey (1991), Relation between alkali volcanism and slab-window formation, *Geology*, **19**, 657–660, doi:10.1130/0091-7613.
- Jadamec, M. A., and M. I. Billen (2010), Reconciling surface plate motions and rapid three-dimensional flow around a slab edge, *Nature*, **465**, 338–342.
- Kincaid, C., and R. W. Griffiths (2003), Laboratory models of the thermal evolution of the mantle during rollback subduction, *Nature*, **425**, 58–62.
- Kneller, E. A., and P. E. van Keken (2008), Effect of three-dimensional slab geometry on deformation in the mantle wedge: Implications for shear wave anisotropy, *Geochem. Geophys. Geosyst.*, **9**, Q01003, doi:10.1029/2007GC001677.
- Lister, G. S., L. T. White, S. Hart, and M. A. Forster (2012), Ripping and tearing the rolling-back New Hebrides slab, *Aust. J. Earth Sci.*, **59**(6), 899–911.
- Long, M. D., and P. G. Silver (2008), The subduction zone flow field from seismic anisotropy: A global view, *Science*, **319**, 315–318.
- Louat, R. (1982), Sismicité et subduction de la terminaison Sud de l'arc insulaire des Nouvelles-Hébrides, *Trav. Doc. ORSTOM*, **147**, 179–185.
- Louat, R., and B. Pelletier (1989), Seismotectonics and present-day relative plate motion in the New Hebrides arc-North Fiji basin region, *Tectonophysics*, **167**, 41–55.
- Louat, R., M. Hamburger, and M. Monzier (1988), Shallow and intermediate depth seismicity in the New Hebrides arc: Constraints on the subduction process, in *Geology and Offshore Resources of Pacific Islands Arcs—Vanuatu Region*, edited by H. G. Greene and F. L. Wong, vol. 8, pp. 279–286, Circum-Pac. Counc. Energy and Miner. Resour., Earth Sci. Ser., Houston, Tex.
- Maillet, P., M. Monzier, J. P. Eissen, and R. Louat (1989), Geodynamics of an arc ridge junction: The case of the New Hebrides Arc/North Fiji Basin, *Tectonophysics*, **165**, 251–268.
- Millen, D. W., and M. W. Hamburger (1998), Seismological evidence for tearing of the Pacific plate at the northern termination of the Tonga subduction zone, *Geology*, **26**, 659–662.
- Monzier, M. (1993), Un modèle de collision arc insulaire-ride océanique. Evolution sismo-tectonique et pétrologique des volcanites de la zone d'affrontement Arc des Nouvelles-Hébrides-Ride des Loyauté, Mémoire de thèse, Univ. Française du Pac.
- Monzier, M., P. Maillet, J. Foyo Herrera, R. Louat, F. Missegue, and B. Pontoise (1984), The termination of the southern New Hebrides subduction zone (southwestern Pacific), *Tectonophysics*, **101**, 177–184.
- Monzier, M., J. Boulouin, J. Y. Collot, J. Daniel, S. Lallemand, and B. Pelletier (1989), Premiers résultats des plongées Nautile de la champagne SUB-SPOI sur la zone de collision "ride des Loyauté arc des Nouvelles-Hébrides" (Sud-Ouest Pacifique), *C. R. Acad. Sci. Paris*, **309**, 2069–2076.
- Monzier, M., J. Daniel, and P. Maillet (1990), La collision "ride des Loyauté/arc des Nouvelles Hébrides" (Pacifique Sud-Ouest), *Oceanol. Acta*, **10**, 43–56.
- Monzier, M., L. V. Danyushevsky, A. J. Crawford, H. Bellon, and J. Cotten (1993), High-Mg andesites form the southern termination of the New Hebrides island arc (SW Pacific), *J. Volcanol. Geotherm. Res.*, **57**, 193–217, Noumea.
- Monzier, M., C. Robin, J. P. Eissen, and J. Cotten (1997), Geochemistry vs. seismo-tectonics along the volcanic New Hebrides Central Chain (Southwest Pacific), *J. Volcanol. Geotherm. Res.*, **78**, 1–29.
- Mortimer, N., P. B. Gans, J. M. Palin, R. H. Herzer, B. Pelletier, and M. Monzier (2014), Eocene and Oligocene basins and ridges of the Coral Sea-New Caledonia region: Tectonic link between Melanesia, Fiji, and Zealandia, *Tectonics*, **33**, 1386–1407, doi:10.1002/2014TC003598.
- Ogg, J. G. (2012), Geomagnetic polarity time scale, in *The Geologic Time Scale 2012*, edited by F. M. Gradstein et al., pp. 85–112, Elsevier, Amsterdam.
- Okal, E. A., and S. H. Kirby (1998), Deep earthquakes beneath the Fiji Basin, SW Pacific: Earth's most intense deep seismicity in stagnant slabs, *Phys. Earth Planet. Inter.*, **109**, 25–63, doi:10.1016/S0031-9201(98)00116-2.

- Pascal, G., B. L. Isacks, M. Barazangi, and J. Dubois (1978), Precise relocations of earthquakes and seismotectonics of the New Hebrides island arc, *J. Geophys. Res.*, **83**, 4957–4973.
- Pelletier, B. (1999), *Subduction de ride et ouverture arrière-arc dans le Pacifique Sud-Ouest (arcs des Tonga-Kermadec et du Vanuatu, bassins de Lau et Nord-Fidjien)*, Mémoire d'Habilitation à Diriger des Recherches, Univ. Paris-6, Villefranche sur Mer.
- Pelletier, B., and R. Louat (1989), Seismotectonics and present day relative plate motion in the Tonga Lau-Kermadec Havre region, *Tectonophysics*, **165**, 237–250.
- Pelletier, B., S. Calmant, and R. Pillet (1998), Current tectonics of the Tonga-Nw Hebrides region, *Earth Planet. Sci. Lett.*, **164**, 263–276.
- Richards, S., R. Holm, and G. Barber (2011), When slabs collide: A tectonic assessment of deep earthquakes in the Tonga-Vanuatu region, *Geology*, **39**, 787–790.
- Schellart, W. P. (2004), Kinematics of subduction and subduction-induced flow in the upper mantle, *J. Geophys. Res.*, **109**, B07401, doi:10.1029/2004JB002970.
- Schellart, W. P., and G. S. Lister (2004), Tectonic models for the formation of arc-shaped convergent zones and back-arc basins, in *Orogenic Curvature: Integrating Paleomagnetic and Structural Analyses*, *Geol. Soc. Am. Spec. Pap.* **383**, pp. 237–258, edited by A. J. Sussman and A. B. Weil, Geol. Soc. Amer.
- Schellart, W. P., G. S. Lister, and M. W. Jessell (2002), Analogue modeling of arc and backarc deformation in the New Hebrides arc and North Fiji Basin, *Geology*, **30**(4), 311–314, doi:10.1130/0091-7613.
- Schellart, W. P., J. Freeman, D. R. Stegman, L. Moresi, and D. May (2007), Evolution and diversity of subduction zones controlled by slab width, *Nature*, **446**, 308–311, doi:10.1038/nature05615.
- Sigurdsson, I. A., V. S. Kamenetsky, A. J. Crawford, S. M. Eggins, and S. K. Zlobin (1993), Primitive island arc and oceanic lavas from the Hunter Ridge-Hunter Fracture Zone. Evidence from glass, olivine and spinel compositions, *Mineral. Petrol.*, **47**, 149–169.
- Smith, G. P., D. A. Wiens, K. M. Fischer, L. M. Dorman, S. C. Webb, and J. A. Hilderbrand (2001), A complex pattern of mantle flow in the Lau Back-arc, *Science*, **292**, 713–716.
- Smith, W. H. F., and D. T. Sandwell (1997), Global seafloor topography from satellite altimetry and ship depth soundings, *Science*, **277**, 1957–1962.
- Tanahashi, M., K. Kisimoto, M. Joshima, P. Jarvis, Y. Iwabuchi, E. Ruellan, and J. M. Auzende (1994), 800 km long N-S spreading system of the North Fiji Basin, in *STARMER Project, Mar. Geol. Spec. Issue*, edited by J. M. Auzende and T. Urabe, pp. 5–24, Elsevier, Amsterdam.
- Tatsumi, Y., and S. Eggins (1995), *Subduction Zone Magmatism*, 211 pp., Blackwell Sci., Cambridge, U. K.
- Taylor, F. W., M. Bevis, B. Schutz, D. Kuang, J. Recy, S. Calmant, D. Charley, M. Regnier, B. Perin, M. Jackson, and C. Reichenfeld (1995), Geodetic measurements of convergence at the New Hebrides island arc indicate arc fragmentation caused by an impinging aseismic ridge, *Geology*, **23**, 1011–1014.
- Thorkelson, D. J., and K. Breitsprecher (2005), Partial melting of slab window margins: Genesis of adakitic and non-adakitic magmas, *Lithos*, **79**, 25–41, doi:10.1016/j.lithos.2004.04.049.
- Thorkelson, D. J., J. K. Madsen, and C. L. Slaggett (2011), Mantle flow through the Northern Cordilleran slab window revealed by volcanic geochemistry, *Geology*, **39**(3), 267–270, doi:10.1130/G31522.1.
- Wessel, P., and W. H. F. Smith (1998), New improved version of the Generic Mapping Tools released, *Eos Trans. AGU*, **79**, 579.
- Wortel, M., R. Govers, and W. Spakman (2009), Continental collision and the STEP-wise evolution of convergent plate boundaries: From structure to dynamics, in *Subduction Zone Geodynamics*, edited by S. Lallemand and F. Funiciello, pp. 47–59, Springer, Springer-Verlag, Berlin Heidelberg.